Eur. Phys. J. D **7**, 317–321 (1999)

THE EUROPEAN PHYSICAL JOURNAL D

EDP Sciences
© Società Italiana di Fisica
Springer-Verlag 1999

Direct measurement of fine structure changing collisional losses in cold trapped ^{85}Rb

L.G. Marcassa, R.A.S. Zanon[a], S. Dutta[b], J. Weiner[c], O. Dulieu[d], and V.S. Bagnato[e]

Instituto de Física de São Carlos, Universidade de São Paulo, Caixa Postal 369, São Carlos SP 13560-970, Brazil

Received 26 October 1998 and Received in final form 2 February 1999

Abstract. Using a technique that consists in ionizing atoms out of the $5P_{1/2}$ fragments originated in the cold collision process, we have measured the contribution of the fine structure changing collision (FS) to the total trap loss rate of cold ^{85}Rb. Our results show that FS contribution is responsible for about 4% of the total trap loss. This result should stimulate new theoretical discussions involving exoergic cold collisions.

PACS. 32.80.Pj Optical cooling of atoms; trapping – 33.80.Ps Optical cooling of molecules; trapping – 34.50.Rk Laser-modified scattering and reactions

1 Introduction

Collisions of cooled and trapped atoms have been extensively investigated both theoretically and experimentally [1,2]. In a magneto-optical trap (MOT), trapping and cooling of atoms are achieved by resonant light forces, making the cold trapped sample be a mixture of atoms in the ground and excited states. If, during an atomic collision, one of the atoms is excited, the atomic pair may end up in an attractive long range $-1/R^3$ potential, producing an acceleration of the atoms towards each other. Because the collision time is comparable to the excited state lifetime, spontaneous emission can take place during the atomic encounter, promoting a sudden change of molecular state together with the emission of a red shifted photon, transferring the internal energy of the system to kinetic motion. If the transferred kinetic energy is high enough to eject the atomic pair from the trap, the process will result in trap loss. The mechanism is referred to as radiative escape (RE). For alkalis, there is also another exoergic process involving excited-ground state collisions. Due to the existence of fine structure in the excited state ($P_{3/2}$ and $P_{1/2}$ levels), the atomic encounter can result in a fine structure changing (FS) collision, with the release of $\Delta E_{\rm FS}$ (energy between the two fine structure levels), which is shared by both atoms in the form of kinetic energy. *E.g.*, the fine structure changing collision in sodium transfers about 12 K of energy to each atom ($\Delta E_{\rm FS}/2$), so that they can easily escape from the MOT, whose depth is typically 1 K.

Earlier investigations in the field of cold collisions examined the importance of collisional losses as a limiting factor for the trap density and provided a measurement of the absolute loss rate constant as a function of light intensity [1]. In the earlier experiments, only the total trap loss rate, which is the sum of RE and FS, has been determined. The only exception is ^{7}Li [3], where the FS delivers an amount of energy smaller than the trap depth and does not cause loss in the normal trap operation. Other experiments involving excitation of the $P_{1/2}$ level of Rb [4] and Na [5] have excluded FS, as well. It is important to distinguish between these two mechanisms, because it allows a more precise comparison with theory, leading to a better understanding of exoergic cold collisions. To our knowledge, there are two studies, where the contributions of RE and FS losses were indirectly measured or observed; one was performed in cesium by Fioretti *et al.* [6] and the other by Wang *et al.* in potassium [7]. In the Cs experiment, the photons of the $6P_{1/2} \rightarrow 6S_{1/2}$ decay were counted and the FS contribution to the total trap loss rate evaluated. Although the authors could not make a direct comparison with the total loss rate in their own experiment, comparison with existent values shows that FS is responsible for less than 25% of the total loss rate in Cs MOT at a total laser intensity of 10 mW/cm^2. FS was directly observed by selective ionization of the $4P_{1/2}$ fragments in the potassium experiment. But no attempt to evaluate the FS contribution to the total loss rate was made based on the results. In our experiment, the FS contribution in ^{85}Rb is measured by direct photoionization of the $5P_{1/2}$ fragments. It is, in principle, similar to the experiment by Wang *et al.* [7], but we extract the FS

[a] *Present address*: Instituto de Química de São Carlos, Universidade de São Paulo and CCT-FEJ, Universidade do Estado de Santa Catarina, Brazil.

[b] *Present address*: University of Michigan, Ann Arbor, USA.

[c] *Present address*: Université Paul Sabatier, Toulouse, France.

[d] *Present address*: Université de Paris-Sud, Orsay, France.

[e] e-mail: `vander@ifsc.sc.usp.br`

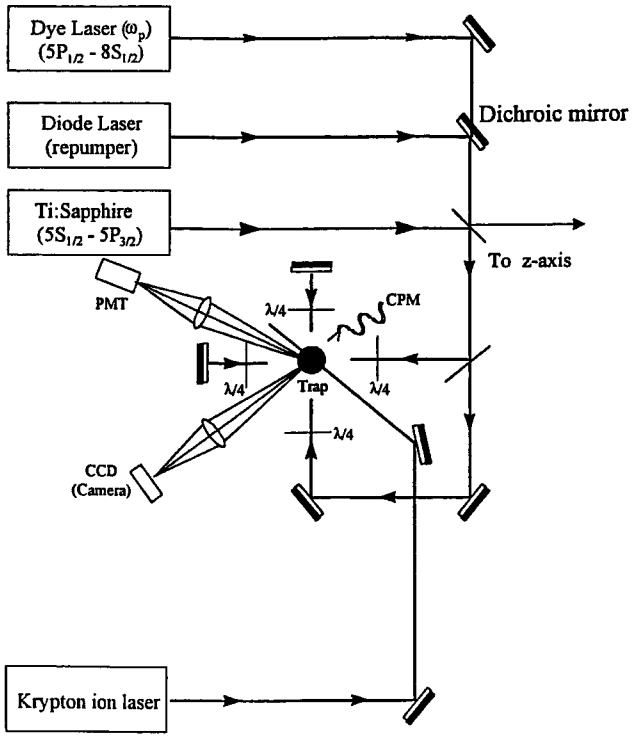

Fig. 1. Experimental setup. Rubidium is trapped in a MOT using a Ti:sapphire laser while a dye laser is tuned to the $5P_{1/2} \rightarrow 8S_{1/2}$ transition and the krypton laser ionizes atoms out of the $8S_{1/2}$ state. A channeltron particle multiplier detects the ions.

contribution to the total trap loss from the results. We have focused our interest on observing the FS contribution in a conventional MOT operating at high power. A full study varying all possible parameters of the trap would be very interesting, but is not the scope of this article.

2 Experimental setup

Figure 1 shows a scheme of the experimental setup. The Rb vapor from a reservoir maintained at -20 °C effuses through a valve into the main chamber maintained at a background pressure of 10^{-10} torr. Three mutually orthogonal, retroreflected laser beams from a Ti:sapphire laser tuned 5 MHz to the red of the atomic $5S_{1/2}(F = 3) \rightarrow 5P_{3/2}(F' = 4)$ transition, intersect at the center of the quadrupole magnetic field generated by a pair of anti-Helmholtz coils. The magnetic field coils are located outside the chamber and produce an axial field gradient of about 10 gauss/cm near the center. A diode laser tuned to the $5S_{1/2}(F = 2) \rightarrow 5P_{3/2}(F' = 3)$ transition works as a repumping. This configuration of static magnetic field and light field, with appropriate laser polarization, creates an environment that traps and cools atoms to about 100 μK. The number of trapped atoms is measured by imaging their fluorescence onto a calibrated photomultiplier (PMT) and the volume of the cloud can be derived from pictures taken with a camera (CCD). These two values are used to calculate the atomic density. A channeltron ion detector (CPM) is positioned 3 cm from the trap center with a bias voltage of about -3 kV applied to the grid in front of the detector, which extracts the produced ions with an efficiency of nearly 100%.

Two additional laser frequencies are irradiated into the chamber. A single mode dye laser (ω_p) is tuned to the transition $5P_{1/2} \rightarrow 8S_{1/2}$ ($\lambda = 616$ nm) and a krypton ion laser beam ($\lambda \sim 640$ nm) is used to ionize the $8S_{1/2}$ state in a near threshold situation. If a FS process takes place, the atoms that emerge in the $5P_{1/2}$ state can be excited and ionized. Finally the ions (Rb^+) are detected.

3 Detection of $P_{1/2}$ fragments

After the FS process, an atom in the $5P_{1/2}$ state leaves the trap with an energy of about 100 K, and an isotropic velocity distribution. Due to this fact, the $5P_{1/2} \rightarrow 8S_{1/2}$ transition will have a Doppler broadening of $\simeq 600$ MHz. If we use the dye laser (typically 1 MHz wide) to excite this transition in only one direction, the number of emerging $P_{1/2}$ atoms in resonance with it will be very small because of the small spectral overlap with the inhomogeneous Doppler profile. Some improvement is achieved by shining the 616 nm laser counter-propagating in three directions. On the other hand, the Doppler broadening is not a problem for the laser that ionizes atoms out of the $8S_{1/2}$ state ($\lambda \sim 640$ nm) because it is already coupled to the continuum.

To be able to access all atoms within the whole Doppler profile, the dye laser ($5P_{1/2} \rightarrow 8S_{1/2}$) is swept through the whole expected frequency range and the ion count rate is integrated in the frequency domain. The signal at frequency ω_p is given by $S(\omega_p) = \int_{-\infty}^{\omega_p} \Phi_{ion}(\omega)d\omega$, with $\Phi_{ion}(\omega)$ being the ion rate at ω. This procedure takes the average over all trajectories and guarantees access to all velocities emerging from the $5P_{1/2}$ state. This integrated signal together with a calibration procedure, allows the determination of the rate for producing atoms in the $5P_{1/2}$ state. A schematic representation for this detection of the $5P_{1/2}$ fragments is presented in Figure 2.

By the fact that the produced $P_{1/2}$ atoms are moving at random directions and illuminated by six laser beams to excite them to the $8S_{1/2}$ state may look rather complicated but it is not really true. Each atom flying out encounters six different laser frequencies. Additionally, those frequencies are scanned through the whole Doppler profile to assure that at least one of them will excite it. This is actually done to maximize the chances of atomic excitation. Finally, the integration over all frequencies adds up all possible trajectories, thereby counting all the atoms.

4 Determination of FS contribution to the total trap loss rate

In the regime of high light intensity and a large number of trapped atoms, the trap loading proceeds essentially at a constant density [8], and the equation which describes the time evolution for the number (N) of trapped atoms

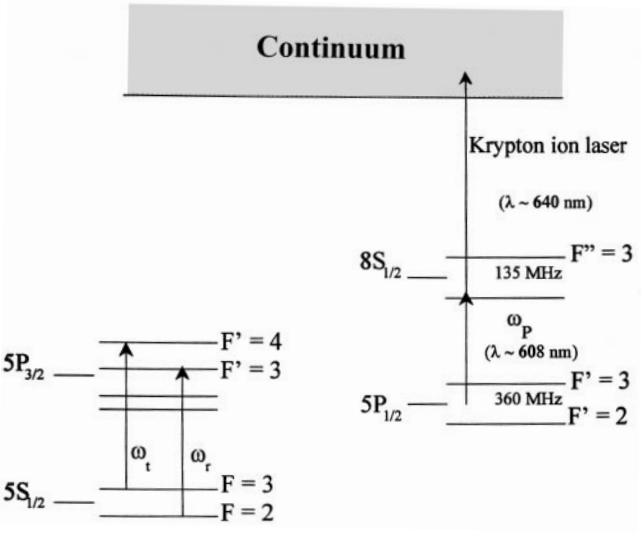

Fig. 2. Schematic diagram showing the atomic levels and the transitions accessed by the lasers in the experiment. On the left hand side we show the transitions for the MOT operation. The transitions shown on the left hand side involving the $8S_{1/2}$ state are used in the detection scheme.

is given by:

$$\frac{dN}{dt} = L - (\gamma + \beta_{\text{total}} n_c) N \qquad (1)$$

where L is the loading rate of atoms into the trap from the background vapor, γ is the loss rate due to collisions between trapped atoms and the background vapor, β_{total} is the total loss rate due to collisions between trapped atoms, and n_c is the density of trapped atoms.

We first determined β_{total} using conventional techniques [8]. In short, the fluorescence of the atoms as a function of time is measured during a loading cycle. Assuming that the fluorescence is proportional to the total number of trapped atoms, we use equation (1) to fit the exponential fluorescence curve. From the fitting we find $\gamma + \beta n_c$. The loss rate (γ) is fixed by the background pressure and obtained by using a procedure similar to the one reported by Marcassa *et al.* [8]. In our case γ has the value $0.007\,\text{s}^{-1}$. After measuring the density n_c, we obtain β_{total}. For the present experimental conditions ($I \simeq 35$ mW/cm^2 is the sum of the intensities of all six trap-laser-beams) and with a density of $n_c \simeq (2.5 \pm 0.5) \times 10^{10}$ cm^{-3}, we obtain $\beta_{\text{total}} = (3.9 \pm 0.8) \times 10^{-12}$ cm^3/s, which is in reasonable agreement with previous measurements [9].

Next, we measure the rate at which the $5P_{1/2}$ atoms are produced. The dye laser (616 nm) is irradiated into three arms of the MOT, creating a total intensity of 318 mW/cm^2 in a Gaussian profile (waist of 5 mm) after the retro-reflection. The krypton ion laser is focused to roughly match the size of the atomic trapped cloud, which corresponds to a total intensity of 2.8 kW/cm^2 at location of the atoms.

In order to take into consideration the ions produced in the background vapor, the trapping and repumping lasers are tuned to the blue side of the atomic resonances (the trapped cloud is then absent) and the integrated ion signal is taken. This background spectrum (see inset of Fig. 3) is constant with frequency, because there is no mechanism pumping atoms into the $P_{1/2}$ state. Therefore, the $S(\omega)$ is almost a straight line. This background signal will be subtracted from the actual spectrum when the cloud is present.

The integrated ion spectrum as function of the dye laser frequency was measured over a 2000 MHz range. This frequency range guarantees that we are connecting all possible hyperfine levels of the $5P_{1/2}$ to the $8S_{1/2}$ state within the Doppler profile of the emerging $5P_{1/2}$ atoms. No variation in the trap fluorescence or size was observed due to the presence of the additional lasers (dye and krypton), which proves that they have no detectable influence on the trap performance. The integrated spectrum with the operating MOT is also shown in the inset of Figure 3. It deviates from the background signal in the region where $P_{1/2}$ atoms are detectable. The difference between these two curves represents the net contribution of FS. In Figure 3 (full size) we have a typical integrated net ion signal as a function of ω_p. The observed signal level increases, in a range of about 600 MHz around the resonance of the $5P_{1/2} \rightarrow 8S_{1/2}$ transition, indicating the production of $5P_{1/2}$ atoms from FS in the MOT. Since those are the integrated signals, their difference reaches a new level and stops increasing when the ions are no longer produced. From this spectrum we derived the total rate of ion production covering the whole Doppler profile to be $\Phi_{\text{ion}} = 180 \pm 10$ ion/s. Of course, this is not the $5P_{1/2}$ rate production, but it is related to it. Let us call the rate at which atoms are produced in the $5P_{1/2}$ state due to FS $\dot{N}_{P_{1/2}}$. To associate the number of ions produced out of the $8S_{1/2}$ state with the total rate of ion production, we have done a calibration procedure, which accounts for all possible decays out of the $8S_{1/2}$ (7P, 6P, 5P and by cascade to 7S, 6S, 5S, 5D and 4D), ionization efficiency, ion detection efficiency, etc. The first step is to determine the effective cross-section for ionization out of the $8S_{1/2}$ state in the presence of the photons flux used in our experiment. In order to achieve this, we used the atoms in the $5P_{3/2}$ state in the MOT and the dye laser to excite them from the $5P_{3/2}$ to $8S_{1/2}$. By measuring the fluorescence from the $8S_{1/2} \Rightarrow 5P_{3/2}$ decay, and from the $5P_{3/2} \Rightarrow 5S_{1/2}$ decay we determine the steady state population in the $8S_{1/2}$ and $5P_{3/2}$. At the same time, we measure the ion rate (I_r) and photon flux (Φ) of the krypton laser. The effective ionization cross section out of the $8S_{1/2}$ state within all the experimental conditions is determined by:

$$I_r = \Phi \sigma_{\text{eff}} N_{8S_{1/2}}. \qquad (2)$$

The measured populations in the $8S_{1/2}$ and $5P_{3/2}$ states were found to be in good agreement with a rate equation calculation involving all intermediate levels. For our conditions, the effective ionization cross section out of the $8S_{1/2}$ state is $\sigma_{\text{eff}} = (2.6 \pm 0.4) \times 10^{-17}$ cm^2. The obtained value is in agreement with the existing theory for this type of ionization [10], which heightens the confidence in the calibration method. The second step is to establish

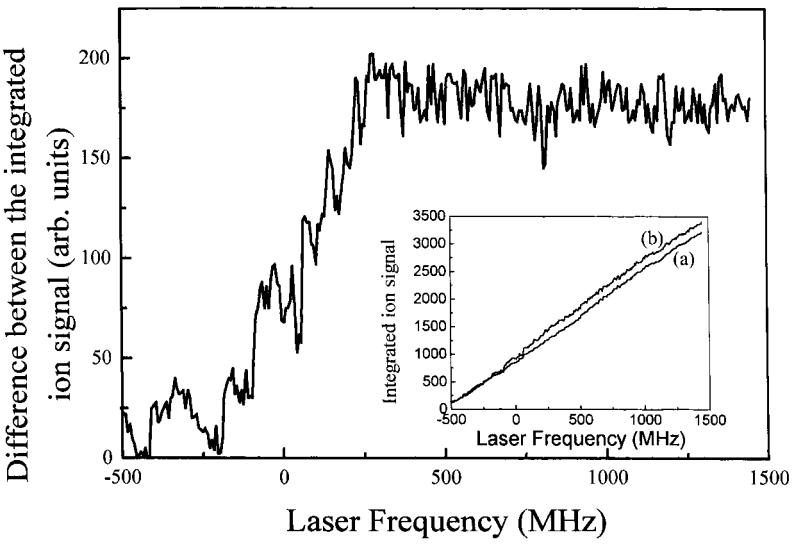

Fig. 3. Integration of the ion spectrum as a function of the dye laser probe frequency. The wide range of rising signal corresponds to the Doppler width of the produced $P_{1/2}$ atoms. In the inset we show both signal that were generated in the presented spectrum: (a) integrated background ion spectrum; (b) integrated ion spectrum during the MOT operation.

a relationship between $\dot{N}_{P_{1/2}}$and $N_{8S_{1/2}}$ (population of the $8S_{1/2}$ state) when the probe laser ($5P_{1/2} \Rightarrow 8S_{1/2}$) is present. This relation is obtained from the rate equation model and reads:

$$N_{8S_{1/2}} = 7.92 \times 10^{-8}(\mathrm{s})\dot{N}_{P_{1/2}}. \quad (3)$$

This is an important step, and at the same time perhaps one of the limitations of this experiment, because it relies on a rate equation model to obtain a relation that is fed back into the experiment. We have thoroughly tested the rate equation model using the background vapor contained in the MOT cell and got similar values for the ionization cross-section, as well as the populations of the $8S_{1/2}$ and $5P_{3/2}$ states. Introducing the result given by equation (3) into equation (2), we can obtain the rate of atoms pumped into $5P_{1/2}$ through:

$$\Phi_{\mathrm{ion}} = 7.92 \times 10^{-8}(\mathrm{s})\Phi\sigma_{\mathrm{eff}}\dot{N}_{P_{1/2}} \quad (4)$$

where Φ_{ion} is the detected ion rate. Considering that each atom produced in $5P_{1/2}$ represents the loss of two atoms from the trap, one can relate the contribution of FS to $\dot{N}_{P_{1/2}}$ by:

$$\beta_{\mathrm{FS}} n_{\mathrm{c}} N = 2\dot{N}_{P_{1/2}}. \quad (5)$$

Using the measured density $n_{\mathrm{c}} = (2.5 \pm 0.5) \times 10^{10}$ cm^{-3} and the measured number of $N = (6.0 \pm 0.5) \times 10^6$ atoms together with $\dot{N}_{P_{1/2}}$ obtained from the equation (4), we calculate $\beta_{\mathrm{FS}} = (0.14 \pm 0.08) \times 10^{-12}$ cm^3/s. Since the total trap loss is the sum of both contributions, $\beta = \beta_{\mathrm{FS}} + \beta_{\mathrm{RE}}$, we can now compare β_{FS} with the total measured loss rate at 35 mW/cm^2 total laser intensity $\beta = (3.9 \pm 0.8) \times 10^{-12}$ cm^3/s. We find that β_{FS} is $(4 \pm 2)\%$ of total β. This result indicates that under the present conditions, radiative escape (RE) is the dominant process for the trap loss in ^{85}Rb and that the fraction of FS is only about 4%. Of course the relative importance of FS may change with trap conditions (laser intensity, detuning, etc.).

5 "Catalysis type" experiment

In order to observe a possible variation of β_{FS} with the laser frequency, we have also carried out a "catalysis type" experiment, by adding an extra frequency from a second Ti:sapphire laser. We have added AOMs (Acoustic Optical Modulators) to the trapping and repumping lasers which allows cycling between the two phases (trapping/probing). We alternate at periods of 50 μs. Controlling the delay between the off-time of the trapping laser and the repumping laser, enabled us to optically pump our sample of cold atom to either $5S_{1/2}(F = 3)$ or the $5S_{1/2}(F = 2)$ ground state. By adding a probe (or catalysis) laser, we observed an additional loss which now allowed for the determination of the frequency dependence in trap loss, without disturbing the trapping phase.

The frequency of the probe laser was tuned from -1000 MHz to -50 MHz and we following the normal procedure in catalysis type experiments [11]. The total intensity of the catalysis laser was 100 mW/cm^2 at -1000 MHz and at the end of the scan (-50 MHz) the intensity was about 5 mW/cm^2. During the whole interval the decrease observed in the number of atoms was about 10%. When the initial hyperfine ground level was $5S_{1/2}(F = 3)$, no variation in the ion rate was observed during the whole frequency tuning range of the catalysis laser, meaning that no changes in β_{FS} were induced by the probe laser. In contrast, starting with $5S_{1/2}(F = 2)$ hyperfine ground state atoms, an increase in the β_{FS} is noted, as the probe laser scans. From the beginning to the end of the catalysis laser scan, the increase in the ion rate production was compatible with an increase on β_{FS} from the original 4% of β to about $(9 \pm 4)\%$ of β. Unfortunately, the catalysis type experiment here performed, was not accurate enough to reveal a dependence of the FS with laser detuning. It shows, however, that the $5P_{3/2} + 5S_{1/2}(F = 2)$ asymptotic potential is more favorable for FS than the one leading to $5P_{3/2} + 5S_{1/2}(F = 3)$.

6 Discussions

Theoretical estimates of trap loss rates, using a variety of semiclassical and quantum models, have been reported previously for all alkali atoms, and have been reviewed by Suominen [12]. They rely on the factorization of the rate into two terms, one describing the excitation of the atom and its survival under spontaneous decay in the long-range part of the collision. The second term accounts for the probability of a short-range process responsible for the trap loss.

According to Dashevskaya *et al.* [13], the FS process for the heavier alkalis (Rb and Cs) is expected to occur mainly at short internuclear distances, where the exchange energy dominates all the other interactions (dipole-dipole, rotational coupling, spin-orbit). In our experiment, the transition occurs through radial coupling at an avoiding crossing between the two attractive 0_u^+ Rb_2 states, one of which dissociates to the $5S_{1/2} + 5P_{3/2}$ and the other to the $5S_{1/2} + 5P_{1/2}$ asymptotic limit. Accurate knowledge of these molecular potentials is required to evaluate the FS transition probability.

In our experiment, the excitation process involves specific hyperfine sublevels: the normal operating mode of the trap populates essentially the $F = 3$ hyperfine level of the ground state atoms, allowing the excitation to the $^2P_{3/2}$ ($F' = F, F \pm 1$) levels. The corresponding potential curves including the hyperfine structure have not been published for Rb_2, but they are qualitatively similar to those calculated for Na_2 [14]: as the 0_u^+ state is the most attractive state within the $S + P_{3/2}$ manifold, it adiabatically and smoothly correlates to the lowest dissociation limit $S(F = 2) + P_{3/2}$. In the normal operating mode of the trap, no significant FS loss is expected to occur, which is in agreement with the measured small upper limit for β_{FS} in our work, as well as with the recent experiment on Cs of Fioretti *et al.* [6].

If the population of the ground state atoms is now transferred from the $F = 3$ to the $F = 2$ level, the 0_u^+ can be efficiently populated by photoexcitation. Despite previous estimates predicting a FS loss rate in the 0_u^+ state as high as 30% of the total loss rate [15], we still do not observe a significant FS loss. Such a discrepancy is also observed in the Cs experiment of reference [6]. Following the discussion of Dulieu *et al.* [16], these disagreements are not so surprising. Indeed, transitions probabilities in atom-atom collisions strongly depend on the details of the molecular potential curves, especially at very low energies. This has been illustrated for FS collision in heavy alkalis in reference [16]. The FS probability can be expressed, in the framework of the Landau-Zener model for the short range pseudocrossing between the 0_u^+ curves, as $P_N^{FS} = 2p_N(1 - p_N)2\sin^2 \Delta_N$. The single passage probability p_N depends on the rotational quantum number N of the relative motion. The transition probability P_N^{FS} is an oscillating function of the difference of phase Δ_N accumulated on each potential curve. As a result, P_N^{FS} is an oscillating function of N. But for cold atoms, only a few values of N are involved in the collision: P_N^{FS} only shows a fraction of a single oscillation with N. The total transition probability P^{FS}, summed over all possible N values, will strongly depend on the detailed shape of this fraction oscillation, or, in other words, $P_{N=0}^{FS}$. In reference [16] it is shown that $P_{N=0}^{FS}$ is extremely sensitive to very tiny changes in the potential curves or in their coupling: for example, the short range repulsive part of the very deep $^3\Pi_u$ potential curve is not known neither from experiment nor from *ab initio* calculations [17], and a shift as small as $0.05a_0$ of the inner turning point of the potential is enough to change $\Delta(N)$ by a significant fraction of π resulting in dramatic variations of $P_{N=0}^{FS}$. The present experimental result suggests that the molecular parameters of the system are such, to induce a small FS probability.

This work has received financial support from FAPESP (Fundação de Amparo à Pesquisa do Estado de São Paulo), CNPq (Conselho Nacional de Desenvolvimento e Pesquisa), and Finep – Núcleos de Excelência (Núcleo de Pesquisa em Óptica Básica e Aplicada).

References

1. P.S. Julienne, A.M. Smith, K. Burnet, Adv. At. Mol. Opt. Phys. **30**, 141 (1993).
2. T. Walker, P. Feng, Adv. At. Mol. Opt. Phys. **34**, 125 (1994).
3. J. Kawanaka, K. Shimizu, H. Takuma, Phys. Rev. A **48**, R883 (1993); N.W. Ritchie, E.R.I. Abraham, Y.Y. Xiao, C.C. Bradley, R. Hulet, P.S. Julienne, Phys. Rev. A **51**, R890 (1995).
4. M.G. Peters, D. Hoffmann, J.D. Tobiason, T. Walker, Phys. Rev. A **50**, R906 (1994).
5. L.G. Marcassa, K. Helmerson, A.M. Tuboy, D.M.B.P. Milori, S.R. Muniz, J. Flemming, S.C. Zilio, V.S. Bagnato, J. Phys. B: At. Mol. Opt. Phys. **29**, 3051 (1996).
6. A. Fioretti, J.H. Müller, P. Verkerk, M. Allegrini, E. Arimondo, P.S. Julienne, Phys. Rev. A **55**, R3999 (1997).
7. H. Wang, P. Gould, W. Stwalley, Phys. Rev. Lett. **80**, 476 (1998).
8. L.G. Marcassa, V.S. Bagnato, Y. Wang, C. Tsao, J. Weiner, O. Dulieu, Y.B. Band, P.S. Julienne, Phys. Rev. A **47**, R4563 (1993).
9. C. Wallace, T. Dinneen, K. Tau, T. Grove, P. Gould, Phys. Rev. Lett. **69**, 897 (1992).
10. M. Aymar, O. Robaux, S. Wane, J. Phys. B: At. Mol. Opt. Phys. **17**, 993 (1984).
11. D. Hoffmann, P. Feng, R.S. Williamson III, T. Walker, Phys. Rev. Lett. **69**, 753 (1992).
12. K.A. Suominen, J. Phys. B: At. Mol. Opt. Phys. **29**, 5981 (1996).
13. E.I. Dashevskaya, A.I. Voronin, E.E. Nikitin, Can. J. Phys. **47**, 1237 (1969).
14. C.J. Williams, P.S. Julienne, J. Chem. Phys. **101**, 2634 (1994).
15. P.S. Julienne, J. Vigué, Phys. Rev. A **44**, 4464 (1991).
16. O. Dulieu, J. Weiner, P.S. Julienne, Phys. Rev. A **49**, 607 (1994).
17. M. Foucrault, Ph. Millié, J.P. Daudey, J. Chem. Phys. **96**, 1257 (1994).